# A Parametric Study on Rotary Slinger Spray Characteristics Using Laser Diagnostics

**Arnab Chakraborty, Mithun Das, Srikrishna Sahu, and Dalton Maurya**

**Abstract** This paper reports an experimental study of spray characteristics in rotary slinger atomizers using different laser diagnostic tools. The main objective of the present study is to investigate the effect of size of the slinger orifices on liquid breakup dynamics and droplet size distribution over a wide range of rotational speed (5000–45,000 rpm) and liquid flow rates (0.2–2 lpm). Three different slinger discs having the same number of orifices but different sizes ($d_0 = 1$, 1.5, and 2 mm) are considered. The primary liquid breakup visualization is achieved using volumetric laser-induced fluorescence (VLIF) technique; whereas, the droplet size is measured by interferometric laser imaging for droplet sizing (ILIDS) technique. The results demonstrate critical role of orifice size on liquid breakup mode and droplet size up to rotational speed about 30,000 rpm, beyond which the aerodynamic force dominates the atomization process such that neither the orifice size nor rate of rotation has strong influence.

**Keywords** Slinger atomizer · Liquid breakup visualization · VLIF · ILIDS · Coriolis force

## Nomenclature

| | |
|---|---|
| AMD | Arithmetic Mean Diameter (μm) |
| Ro | Rossby Number |
| $Q_l$ | Total liquid feed rate (lpm) |
| $D$ | Droplet size (μm) |

A. Chakraborty (✉) · M. Das · S. Sahu
Thermodynamics and Combustion Engineering Laboratory, Department of Mechanical Engineering & National Centre for Combustion Research and Development (NCCRD), IIT Madras, Chennai, Tamil Nadu, India
e-mail: junestar66@gmail.com

D. Maurya
Gas Turbine Research Establishment (GTRE), Bangalore, India



G. Sivaramakrishna et al. (eds.), *Proceedings of the National Aerospace Propulsion Conference*, Lecture Notes in Mechanical Engineering,
https://doi.org/10.1007/978-981-19-2378-4_36

| | |
|---|---|
| $d_0$ | Diameter of slinger orifice (mm) |
| $d_p$ | Diameter of the injection port on liquid delivery manifold (0.7 mm) |
| lpm | Litres per minute |
| $N$ | Rotational speed of slinger (rpm) |
| VLIF | Volumetric Laser Induced Fluorescence |
| $R_0$ | Radius of the slinger disc (45 mm) |
| ILIDS | Interferometric Laser Imaging for Droplet Sizing |

## 1 Introduction

A rotary slinger atomizer in an annular combustor has been frequently used in small-size gas turbines, for instance, in Teledyne's J-69 and Turbomeca's Marbore engines. Simple design and low-cost are the advantages of such atomizer. In addition, importantly, it operates at lower injection pressure compared to pressure atomizer. For maximum power output of a turbine, slinger may be operated at higher rotational speed and it can exceed about 100,000 rpm. But at ideal or relight conditions, the rotational speed is typically in the range of 5000–20,000 rpm. The rotary atomizer is coupled to the turbine shaft and rotates at the shaft speed. The fuel from the pump is fed to discharge orifices on the periphery of the rotary disc. The orifice channels of the disc are drilled in radial or radial-axial direction with respect to the engine shaft. Due to the large centripetal acceleration, the liquid spreads along the inner walls of the atomizer cavity and form a liquid film that supplies the liquid into the orifice channels. Finally, the liquid is discharged from the orifices into the ambience, and it atomizes into droplets forming a spray around the slinger disc. As for any other atomizer, the size of liquid exit area (in the present case the diameter of slinger orifices) is an important design parameter that may strongly influence atomization behaviour, the study of which is the aim of the present paper.

Several studies have reported liquid breakup dynamics in the slinger atomizers. Dahm et al. [1] reported liquid breakup visualization in slinger atomizers for different sizes and shapes of orifices or holes over a wide range of rotational speeds. They stated film and stream modes of liquid injection through for each orifice. The injected film or stream undergoes various types of breakups depending on rotational speed of the disc and geometry of the orifice including subcritical and supercritical mode of breakup for film mode injection. The subcritical breakup refers to the collapse of the annular film, due to surface tension, to form a steam, while the supercritical breakup refers to direct disintegration of the liquid sheet at the orifice exit. The same group [2] conducted a theoretical analysis to predict liquid film thickness, jet diameter for circular as well as non-circular slinger orifice geometry based on film Reynolds number and aerodynamics Weber number, mass and momentum flux of the emerging liquid jet. The authors proposed a correlation for Sauter mean diameter (SMD) in terms of Weber number and Ohnesorge number. The droplet size data measured by Morishita [3] was used for this purpose. Choi et al. [4] performed

series of experiments using high-speed flow visualization and Phase Doppler Particle Analyser for droplet sizing. They considered three different orifice sizes and different arrangements of the orifices on the disc periphery. The experiments were performed in the speed range of 5000–40,000 rpm for a constant liquid mass flow rate. The subcritical mode of liquid breakup is observed up to 15,000 rpm while supercritical mode is observed to be predominant above 30,000 rpm. Droplet sizing measurements were done within 50 mm distance from the slinger disc surface. It is observed that liquid film thickness as well as the SMD decreases with increase in slinger rotational speed. SMD decreased with increase in orifice size. They proposed a linear correlation between SMD and liquid film thickness inside the injection orifice. Though atomization and spray characteristics in slinger atomizers have been studied by a number of other researchers in the past [5–9], they considered same size of orifices for all experiments.

The previous studies mostly used in direct photography for visualization of the liquid breakup process in slinger atomizers. However, the quality of the images degrades for high rotational speed and/or liquid flow rates. This can be overcome by the application of the volumetric laser induced fluorescence (VLIF) technique that allows objective way of visualization of the liquid core region, while the background and also products of atomization around the liquid core (especially for dense sprays) are filtered out. The present paper aims to investigate primary liquid breakup dynamics and spray characteristics in slinger atomizers having different orifice size, which has not gained much attention in the past. The experiments were performed in a high-speed slinger test rig designed to operate over a wide range of conditions. Different laser diagnostic tools were employed in the present work. The visualization of the liquid breakup is achieved by using the VLIF technique, which is advantageous over conventional method of direct imaging as explained above. The size of the spray droplets is measured by interferometric laser imaging for droplet sizing (ILIDS) technique. In the current work, the liquid breakup visualization experiments were performed for the slinger rotational speed in the range 5000–45,000 rpm and the liquid flow rate was varied in the range 0.2–2 lpm.

## 2 Experimental Set-up

A schematic of the slinger atomizer test rig is shown in Fig. 1. The unique slinger rig facility is housed at NCCRD, IIT Madras and comprises following key units.

(a) **Slinger test rig**

The slinger test bed consists of a heavy cast iron test bed with vibration absorber pads at its bottom. The high-speed drive is installed on a heavy test bed that dampens any vibrations during slinger operation. Moreover, a vibration sensor (range: 0–25 mm/s) was installed on the electric drive to monitor the performance of the slinger assembly especially for higher range of rotational speeds of the slinger disc. For all experimental conditions, the recorded vibration limit

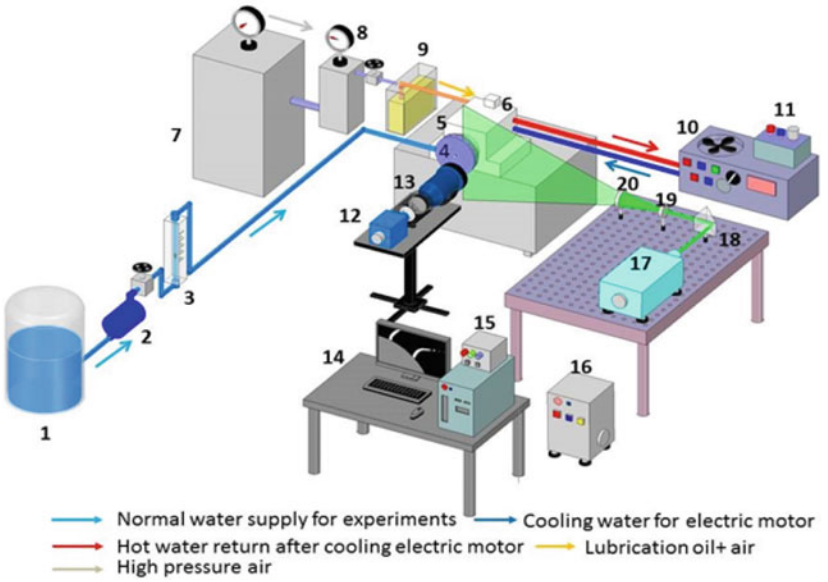


**Fig. 1** Schematic of the slinger atomizer experimental set-up for VLIF experiment. *1.* Water tank, *2.* Pump, *3.* Rotameter, *4.* Slinger disc, *5.* Liquid injection manifold, *6.* Electric drive, *7.* Air compressor, *8.* Air strainer, *9.* Lubrication oil chamber, *10.* Cooling unit, *11.* Frequency controller for electrical drive, *12.* CCD camera, *13.* Macro lens, *14.* Data collection system, *15.* Synchronizer, *16.* Power box for laser, *17.* Nd:YAG laser, *18.* $90^0$ beam deflection prism, *19.* Cylindrical lens and *20.* Spherical lens

was always less than 1 mm/s that ensured smoother and safer operation as per the standard for mechanical vibration. The motor shaft is connected to the shaft of the slinger atomizer, which is a circular titanium disc (radius, $R_0 = 45$ mm) containing 18 number of orifices on its outer periphery (Fig. 2). The liquid is delivered to the slinger disc via a liquid delivery manifold which contains 12 numbers of injection ports uniformly distributed over its periphery (Fig. 2 presents a schematic of the manifold). The diameter of each port is 0.7 mm. The purpose of the manifold is to evenly distribute the liquid to the inner side of the slinger. The liquid (water in the present case) is pumped to the liquid intake line of the manifold (as shown in the Fig. 1) via a rotameter connected to a regulating valve. The liquid goes into the manifold cavity and comes out through the injection ports as liquid jets that impinge on the inner surface of the slinger disc and create a liquid film that serves as a dynamic source of liquid supply. However, it is important to mention that the liquid impingement velocity at any higher liquid feed rate is 40–400 times smaller than the tangential velocity of the slinger disc. Thus, the possibility of liquid jet impingement causing splashing on the inner surface of the disc is minimal. In the present study, three slinger discs (A, B and C) with the same three slinger discs with the same number of orifices but different size of orifices, viz. 1, 1.5 and 2 mm,

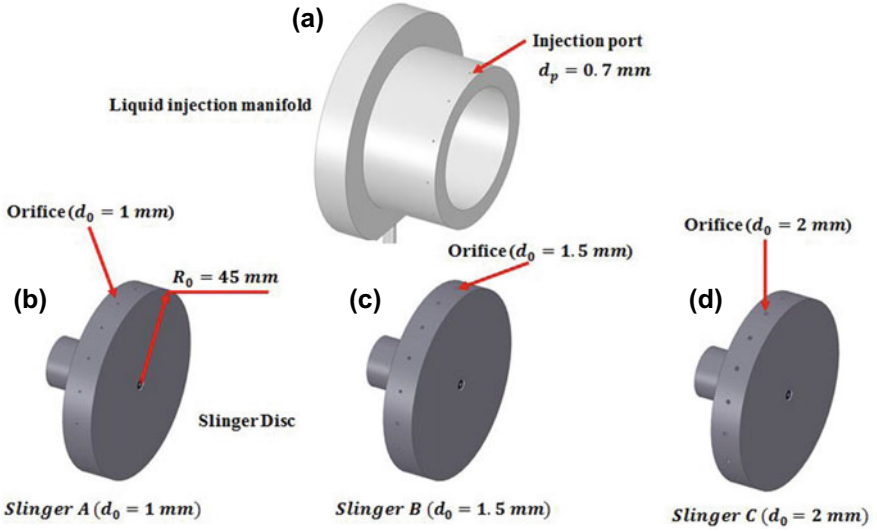


**Fig. 2** **(a)** Liquid injection manifold, **(b)** Slinger A ($d_0 = 1$mm), **(c)** Slinger B ($d_0 = 1.5$mm) and **(d)** Slinger C ($d_0 = 2$mm)

**Table 1** Details of the three slinger discs in present set-up

| Parameters | Slinger A | Slinger B | Slinger C |
|---|---|---|---|
| Diameter of each orifice ($d_0$) | 1 mm | 1.5 mm | 2 mm |
| Number of orifices ($N_s$) | 18 | 18 | 18 |
| Radius of the disc ($R_0$) | 45 mm | 45 mm | 45 mm |
| Length of each orifice ($l$) | 2 mm | 2 mm | 2 mm |

are used (Fig. 2). The details of the slinger discs are summarized in Table 1. At any particular rotational speed of the disc, the liquid in the inner surface of the disc is ejected out of each of the slinger orifices and atomizes as it interacts with the surrounding air, However, as the liquid flows through each of the slinger orifice, it may not fill its inner surface of the orifice completely, and in such case, the liquid film is not uniformly distributed inside each orifice. The slinger rotational speed $N$ was varied in the range 5000–45,000 rpm, and the liquid flow rate $Q_l$ was in the range from 0.2 to 2 lpm.

(b) **Lubrication unit**

The lubrication unit ensures supply of oil from the lube oil chamber to the bearings of the high-speed drive for appropriate lubrication which is essential for smooth running of the slinger disc.

(c) **Cooling unit**

During the rotation of moving components such as shaft and bearing, heat generation due to friction raises the temperature of associated parts, which

needs to be lowered for hassle-free and safe operation. This is done by the cyclic circulation of the cool water through the heat exchanger.

Now we discuss the application of different laser-based techniques for the atomization and spray study in the current work. In the present work, the primary liquid breakup is visualized using volumetric laser-induced fluorescence (VLIF) technique (Fig. 1); whereas, the droplet size measurement is obtained using interferometric laser imaging for droplet sizing (ILIDS) technique as discussed below.

## 2.1 VLIF-Based Visualization of Liquid Breakup

In VLIF optical arrangement, a single pulse Nd: YAG laser (Quantel: Q-smart 850, 532 nm, 5 ns pulse width and 6.5 mm beam diameter) was used as the illuminating source. A cylindrical lens (focal length: −25 mm) and a spherical lens (focal length: +250 mm) were used to convert the laser beam to a sheet (height 5 cm and beam waist about 1–2 mm). The thickness of the laser sheet was adjusted while using slinger discs with different orifice sizes to ensure that the laser illuminates the whole orifice for all cases. The laser is synchronized with a CCD camera (PCO Pixelfy, 1040 × 1392 pixel2, 14-bit and 13.5 Hz) using an Arduino board. In total, 400 images were captured using a 150 mm macro lens (Sigma, f/2.8). In this technique, adequate amount of Rhodamine 6G is uniformly mixed in water tank, then the water tagged with the dye is fed into the slinger during experiment. Upon illuminated by the green laser, the liquid absorbs the incident irradiation and fluoresces at the red-shifted light (with peak around 555 nm) which is captured by the camera equipped with a bandpass filter (550 ± 10 nm). Thus, the scattered light is rejected and only the fluorescent liquid core is imaged. This way the signal to noise ratio is high, and very good quality images with high background contrast is imaged. In order to highlight the advantage of the VLIF technique, we compare a VLIF image with front light illuminated image in Fig. 3 for the same operating condition of $Q_l = 2$ lpm and at $N = 30{,}000$ rpm for slinger disc B, as example. The above figure clearly demonstrates the potential of the VLIF technique, while the direct imaging suffers from poor contrast due to hindrance of light by the droplets around the liquid core so that imaging of the latter is very difficult. Nevertheless, for lower range of liquid flow rate and rotational speed, direct photography provides reasonably good images.

## 2.2 Droplet Sizing by ILIDS

The optical arrangement for application of ILIDS in the present experiments has been presented in Chakraborty and Sahu [10], Sahu et al. [9], and hence not repeated here. The same laser and sheet optics as mentioned earlier for VLIF technique were employed. The CCD camera was also same, although the optical setting for

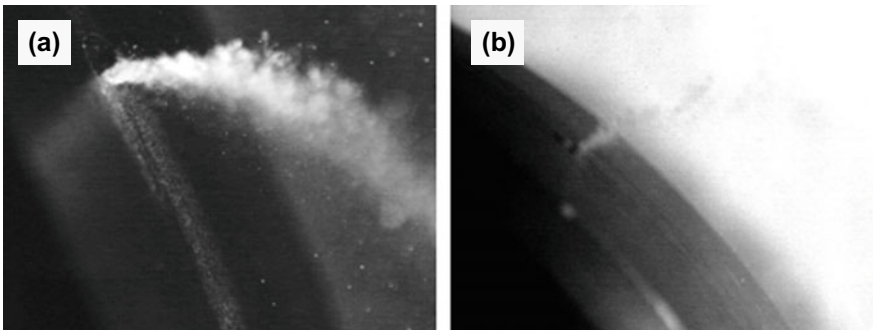


**Fig. 3** **(a)** A sample VLIF image, (**b**) an image acquired by front light illumination using a stroboscope for $Q_l = 2$ lpm and at $N = 30{,}000$ rpm and Slinger B

ILIDS imaging system was different. The camera was oriented at the forward scattering angle, $\theta = 69°$ (optimum angle for maximum interference while using water droplets). A 105 mm Nikon lens (f/2.8) was used to collect the scattered light. An optical compression unit (a pair of cylindrical lenses), positioned in between the CCD camera and the lens, compresses the circular fringe pattern from a droplet such that each droplet is finally imaged as a rectangular region with superposed fringes. A rectangular aperture (30 × 2 mm) was mounted on the lens to control the collecting angle, $\alpha$, which was about 8° in the present case. The entire imaging system assembly was housed on a custom-made frame that also incorporates the Scheimpflug mount for the camera due to which the degree of defocusing remain almost same across the image (i.e. otherwise not possible due to non–90° viewing in ILIDS). In the next step, the ILIDS images were processed to obtain droplet size, which is expressed as given below [11],

$$D = \frac{\lambda}{\alpha}\left(\cos\left(\frac{\theta}{2}\right) + \frac{m\sin\left(\frac{\theta}{2}\right)}{\sqrt{m^2 - 2m\cos\left(\frac{\theta}{2}\right) + 1}}\right)^{-1} n \tag{1}$$

where $\lambda$ is the wavelength of the laser light and $\alpha$ is the collecting angle of the receiver. The above equation can be written as, $D = \kappa n$, where $\kappa$ is an experimental constant that represents droplet diameter per fringe and is given by the bracketed term in Eq. 1. In the present experiments, $\kappa$ was about 3 $\mu$m/fringe. The details of the ILIDS image processing could be found out in Manish and Sahu [12], Boddapati et al. [13]. The application of the ILIDS technique for droplet size measurement in slinger atomizers has been demonstrated in our earlier study [10].

The ILIDS images were captured at the radial station at $R = 2R_0$ ($R_0$ is radius of slinger disc and equals to 45 mm) away from the slinger surface. The selection of the measurement plane is not arbitrary. Lee et al. [14] carried out combustion study in rotary atomizer of disc diameter of 40 mm, and they reported that the reaction zone

of combustion zone is within 50 mm distance away from the outer disc periphery. Accordingly, in the current study, the spray characteristics are decided to be measured at $2R_0$ location. For each experiment, 1000 ILIDS images were captured that ensured statistical convergence of the measured characteristic size of spray droplets. For $Q_l =$ 0.2 lpm, the droplet sizing experiments were conducted up to $N = 45{,}000$ rpm. The characteristic droplet diameter is represented as arithmetic mean diameter (*AMD*) in the present study and defined as given by the expression;

$$\text{AMD} = \frac{\sum_1^n N_i D_i}{\sum_1^n N_i},$$

where $N_i$ is the number of droplets in the size class represented by droplet size $D_i$ and '$n$' is the total number of images.

## 3 Result and Discussions

### *3.1 Liquid Breakup Morphology*

The liquid breakup images close to the orifice exit are presented in Figs. 4 and 5 for $Q_l = 0.2$ and 2 lpm, respectively, for different rotational speeds. For each case, the images are shown for the three atomizers, i.e. slinger disc A, B and C (corresponding to orifice size, $d_o = 1$ mm, 1.5 mm and 2 mm, respectively). Before we discuss the influence of orifice size, some common observations are noted.

(i) For each case, the primary breakup zone of the liquid, which is characterized by unbroken liquid length, is observed. The liquid, as it exists from the orifice, interacts with the surrounding air, which can be considered to approach the liquid (from the slinger reference frame) in cross-stream manner. Due to aerodynamic interaction with the air, the liquid breaks up when the disrupting forces dominate the surface tension forces.

(ii) It is interesting to notice that for all rotational speeds and liquid feed rates, the liquid within an orifice channel is pushed to the side opposite to the direction of slinger rotation despite of having low aspect ratio of the orifice which is unique observation in the present study. This is attributed to the dominant role played by the Coriolis acceleration that tends to accumulate all liquid to one side of the channel as soon as the liquid enters the orifice. As a direct consequence of this, the liquid breakup mode is different in comparison with the case where the liquid exists all along the channel wall [1, 2]. Depending on the operating condition as well as slinger orifice size, broadly three different modes are observed, viz. stream-, transition- and film- modes depending on the structure of the liquid at the orifice exit.

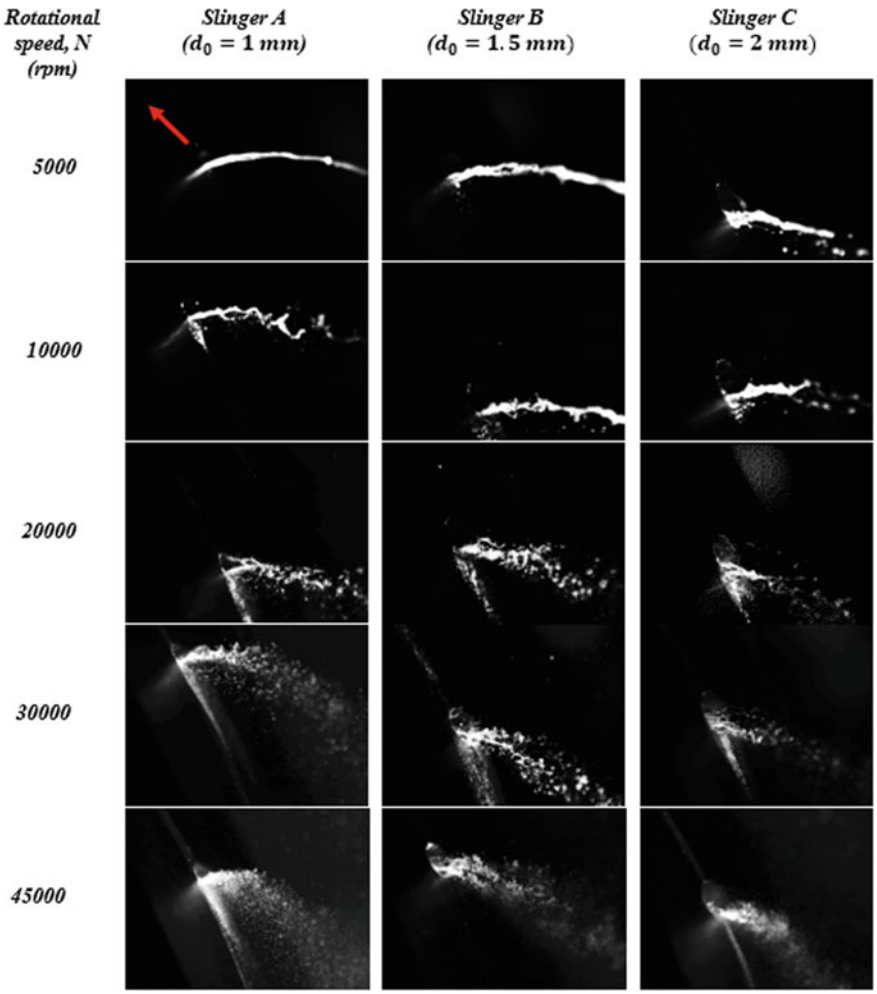


**Fig. 4** Liquid breakup morphology for different size orifice in slinger atomizer over rotational speed of 5000–45,000 rpm at liquid feed rate, $Q_l = 0.2$ lpm. The arrow indicates the direction of rotation of the disc

(iii) As the slinger speed is made higher at the same liquid feed rate (compare images column-wise in Figs. 4 and 5), the breakup length appears to decrease, which is as expected, due to higher velocity of approach of the air flow. It is important to mention here that, due to oblique view, it is not possible to quantitatively indicate the breakup length and only qualitative comparison for different rotational speed and liquid feed rate can be made. Since the VLIF technique provides images with high background contrast, identifying the breakup point is less ambiguous. In addition, due to the same reason, for higher rotational speed (and the same $Q_l$) the liquid breakup structure in the

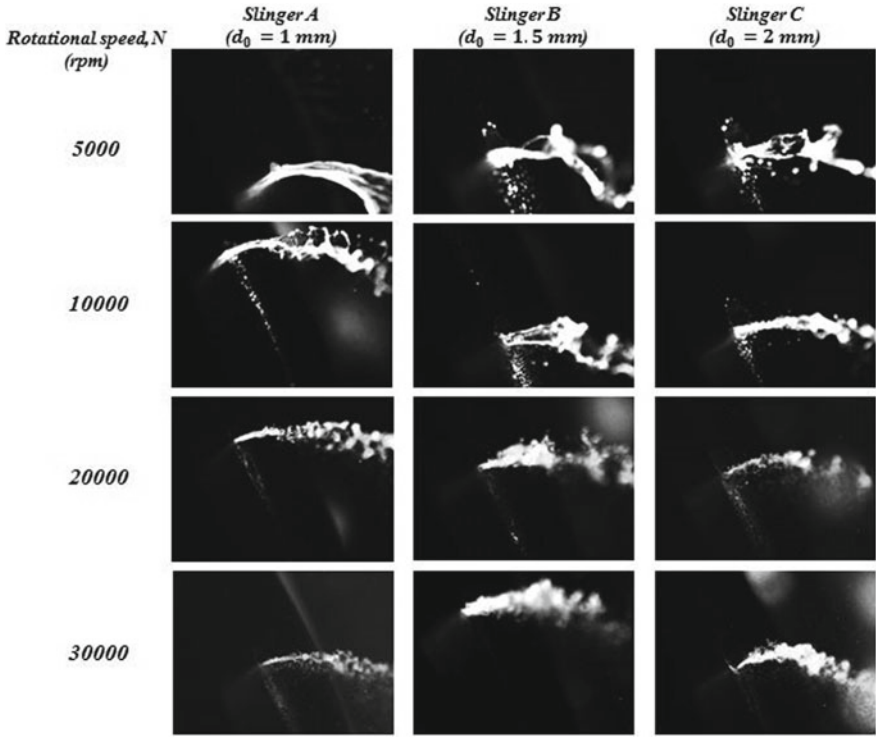


**Fig. 5** Liquid breakup morphology for different size orifice in slinger atomizer over rotational speed of 5000–30,000 rpm at liquid feed rate, $Q_l$ = 2.0 lpm

vicinity of an orifice changes from stream mode to sheet mode. Accordingly, the liquid breakup morphology away from the orifice changes from column breakup regime (at lower $N$) to sheet-, sheet-ligament multi-mode regime and sheer regime at higher $N$.

(iv) As the liquid feed rate is made larger at the same speed (compare images for each case between Figs. 4 and 5), no general trend can be observed as the difference is dependent on the orifice size, as will be discussed later. In general, the liquid is wider at the orifice exit in Fig. 5 compared with Fig. 4. However, no significant difference in either breakup length or regime is evident.

In spite of the above common observations, which demonstrate the key roles of slinger speed and liquid feed rate, some striking influence of orifice size is also observed in the present experiments as explained below.

Even if the slinger speed and liquid feed rate are held constant, comparing the images row-wise either in Figs. 4 or 5, it can be noticed that the liquid breakup length is always larger for $d_o = 1$ mm, followed by $d_o = 1.5$ and 2 mm. In addition, interestingly, for lower range of $N$ (up to about 20,000 rpm), the liquid mode changes from stream mode for $d_o = 1$ mm to film mode for $d_o = 2$ mm. This highlights the

role of curvature of the orifice channel such that smaller orifice leads to stronger effect of surface tension that tends to roll up the liquid resulting in the liquid to exit as a stream. It is worth to mention here that both Coriolis and surface tension forces influence the mode of liquid delivery within a slinger orifice. In fact, the balance between the above forces dictates the thickness and the width of the liquid. However, the curvature of the inner surface of the orifices aids to surface tension force even if the working liquid is the same. Hence, we attributed the observed difference to increased surface tension force. For larger orifice, the liquid is able to spread in the cross-stream direction due to which the liquid exits as a film. As a consequence, the breakup regime of the liquid varies with the diameter of the orifice for the same speed and liquid flow into the atomizer. For example, considering the case $N = 5000$ rpm and $Q_l = 0.2$ lpm in Fig. 4, column breakup corresponding to Rayleigh regime is evident for $d_o = 1$ mm, while a combined sheet-ligament regime occurs for $d_o = 1.5$ mm (ligaments of liquid appear on the boundary of the sheet), on the other hand, the sheet transforms into a bag structure that further breakups for $d_o = 2$ mm. For higher slinger speed ($N > 20{,}000$ rpm), the liquid breakup mode and regime are mostly governed by aerodynamic force, thus, the influence of orifice size is smaller. Overall, the current visualization images indicate that even if the slinger operating conditions are held same, and the liquid never fills up the orifice channel, smaller orifice size leads to poor atomization and vice versa. Though, no much difference in breakup morphology is observed between $d_o = 1.5$ and 2 mm.

Figure 6 presents the droplet size distribution measured at $R = 2R_o$ location for different slinger discs at $Q_l = 0.2$ lpm for the rotational speed range of 10,000–45,000 rpm. As the rotational speed of the disc is made higher for the same liquid feed rate, the size distribution is slightly shifted to left indicating production of smaller droplets. Thus, large numbers of smaller droplets are generated for higher rotational speed, as expected, due to improved atomization. However, an interesting trend is observed comparing the plots for different slinger discs in each subfigures in Fig. 6. For the same speed and liquid feed rate, the droplet size distribution is populated with smaller droplets as the orifice size increases from disc A to disc C. It can be observed that up to $N = 30{,}000$ rpm, as the orifice size is made larger, the probability of smaller droplets is higher and larger droplets is smaller. For very high rotational speed for instance, $N = 45{,}000$ rpm, the droplet size distribution for all slinger discs nearly overlaps. This is further highlighted in the *AMD* vs *N* plots shown in Fig. 7. For all discs, *AMD* reduces with rotational speed. Similar observations are reported by Rezayat and Farshchi [15], Choi and Jang [4] and Chakraborty and Sahu [10]. For a given rotational speed, the trend of AMD with orifice size appears non-monotonic. This is evident especially for $N < 35{,}000$ rpm and requires further investigation to relate droplet size with the observed liquid breakup mode. However, for high rotational speed ($N > 35{,}000$) no significant difference in droplet size for different discs are evident, which is attributed to rigours liquid atomization which is nearly independent of boundary conditions at the orifices (see last row of images in Fig. 4). We note that we have verified the above for different liquid flow rates and speed up to 1 lpm and 10,000 rpm and found that the feed rate does not influence

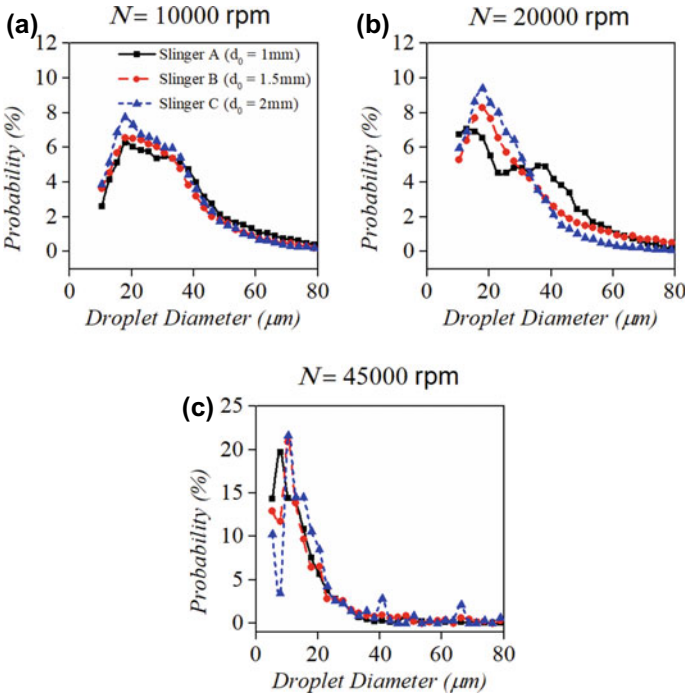


**Fig. 6** Probability distribution of droplet size measured at $R = 2R_o$ location for different slinger discs at rotational speed of (**a**) 10,000 rpm, (**b**) 20,000 rpm, and (**c**) 45,000 rpm at liquid feed rate, $Q_l = 0.2$ lpm

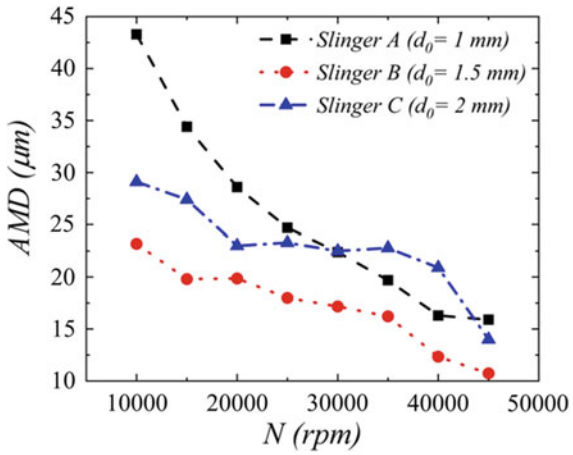


**Fig. 7** Droplet size (*AMD*) variation with rotational speed ($N$) at liquid feed rate $Q_l = 0.2$ lpm for different slingers

much the resulting droplet size. However, further experiments are being conducted currently for higher speed and feed rate.

The above trends for the droplet size and especially the role of orifice size can be explained considering the liquid breakup regimes discussed earlier for the current range of slinger operating conditions. For slinger disc A, Rayleigh type breakup occurs corresponding to the column breakup regime, as a result, the droplet size is of the order of the size of the columns. In contrast to the prevailing sheet and/or ligament breakup regime in disc B and C, the droplet size is smaller. However, at very high rotational speed such as $N = 45{,}000$ rpm, shear breakup is the dominating mode of breakup, and hence, mostly very small droplets are generated for all orifices with different size.

## 4 Conclusion

The motivation behind the present work is to investigate the effect of orifice size on liquid atomization and spray characteristics in slinger atomizers using different laser diagnostic tools. The present study demonstrates the potential application of VLIF technique for visualization of liquid breakup process near the slinger orifices, as high contrast images are obtained in comparison with direct photography. The ILIDS technique was used to measure droplet size. The visualization images demonstrated the dominant role of Coriolis-induced liquid breakup behaviour which means that the liquid in an orifice channel is pushed towards the side opposite to the direction of rotation. It was found that, up to about 30,000 rpm, for the same rotational speed and liquid feed rate, the mode of liquid flow (stream- or film- mode), breakup regime (column-, sheet- or ligament- breakup) and droplet size distribution vary with the size of the orifice channels. Smaller orifice size ($d_o = 1$ mm) promotes column mode liquid transport in the orifice that results in Rayleigh type breakup leading to generation of large-size droplets. Larger orifices ($d_0 = 1.5$ and 2 mm) lead to film mode and sheet and/or ligament breakup regime which is responsible for small droplets in the spray size distribution. The results highlight that smaller the orifice size, larger is the *AMD*. At very high speed such as $N = 45{,}000$ rpm, shear breakup regime was observed for all slinger discs, and also *AMD* does not vary much with the diameter of the slinger orifices.

**Acknowledgements** The authors would like to acknowledge the financial support from the Centre for Propulsion Technology (CoPT), Govt. of India. The authors wish to thank Mr. Thileepan P for his assistance during the design and development of the slinger test rig.

## References


1. Dahm WJA, Patel PR, Lerg BH (2006) Experimental visualizations of liquid breakup regimes in fuel slinger atomization. Atom Sprays 16(8):933–944
2. Dahm WJA, Patel PR, Lerg BH (2006) Analysis of liquid breakup regimes in fuel slinger atomization. Atom Sprays 16(8):945–962
3. Morishita T (1981) A development of the fuel atomizing device utilizing high rotational speed. In: Aircraft engine; marine; turbomachinery; microturbines and small turbomachinery, March 1981, vol 1. American Society of Mechanical Engineers, New York, pp 1–6
4. Choi SM, Jeong JH (2010) Spray behavior of the rotary atomizer with in-line injection orifices. Atom Sprays 20(10):863–875
5. Choi SM, Yun S, Jeong JH, Corber A (2012) Spray in cross flow of a rotary atomizer. Atom Sprays 22(2):143–161
6. Sescu C, Kucinschi BR, Afjeh AA, Masiulaniec KC (2011) Experimental test rig with results on liquid atomization by slinger injectors. J Eng Gas Turbines Power 133(11):210–213
7. Rezayat S, Farshchi M, Karimi H, Kebriaee A (2018) Spray characterization of a slinger injector using a high-speed imaging technique. J Propul Power 34(2):469–481
8. Rezayat S, Farshchi M, Ghorbanhoseini M (2019) Primary breakup dynamics and spray characteristics of a rotary atomizer with radial-axial discharge channels. Int J Multiph Flow 111:315–338
9. Sahu S, Chakraborty A, Maurya D (2020) Coriolis-induced liquid breakup and spray evolution in a rotary slinger atomizer: experiments and analysis. Int J Multiph Flow 135(2021):103532
10. Chakraborty A, Sahu S (2019) Liquid atomization in a high-speed slinger atomizer. In: Volume 1: compressors, fans, and pumps; turbines; heat transfer; structures and dynamics. American Society of Mechanical Engineers
11. Glover A, Skippon S, Boyle R (1995) Interferometric laser imaging for droplet sizing: a method for droplet-size measurement in sparse spray systems. Appl Opt 34:8409–8421
12. Manish M, Sahu S (2019) Droplet clustering and local spray unsteadiness in air-assisted sprays. Exper Therm Fluid Sci 100:89–103
13. Boddapati V, Manish M, Sahu S (2020) A novel approach for conditional measurement of droplet size distribution within droplet clusters in sprays. Exp Fluids 61:42
14. Lee DH, Kim HM, Park PM, You GW, Paeng KS (2009) Full rig test and high-altitude ignition test of micro turbojet engine combustor. In: Proceedings of 2009 KSPE spring conference. The Korean Society of Propulsion Engineers, Daejeon, pp 373–376
15. Rezayat S, Farshchi M (2019) Spray formation by a rotary atomizer operating in the coriolis-induced stream-mode injection. Atom Sprays 29(10):937–963